

relating the solution at t_2 to that at t_1 . These properties of the equations are the basis of the generalized cross section of Head, Humble, Clarebrough, Moreton & Forwood (1973) which considerably speeds up the calculation of dislocation images.

APPENDIX B

The equations relating the amplitudes are

$$\frac{d\psi'(z)}{dz} = B'(z) \psi'(z) + S(z) \exp(-iq_z z) \psi(z) \quad (B1)$$

$$\frac{d\psi(z)}{dz} = B(z) \psi(z), \quad (B2)$$

where the elements of $B(z)$ are

$$\sum_g C_g^i C_g^j \frac{\mathbf{g} \cdot \mathbf{du}(\mathbf{r})}{dz} \exp[i(k^j - k^i)z]$$

and scattered states are denoted by primed quantities:

$$\frac{d[G'(z) \psi'(z)]}{dz} = G'(z) S(z) \exp(-iq_z z) \psi(z) \quad (B3)$$

$$[G'(z) \psi'(z)]_0^T = \int_0^T G'(z) S(z) \exp(-iq_z z) \psi(z) dz \quad (B4)$$

$$\begin{aligned} \psi'(T) &= G'^{-1}(T) G'(0) \psi'(0) + G'^{-1}(T) \\ &\quad \times \int_0^T G'(z) S(z) \exp(-iq_z z) \psi(z) dz. \end{aligned} \quad (B5)$$

As no inelastic scattering takes place before the fast electron enters the crystal $\psi'(0) = 0$ and, using (A6),

$$\psi'(T) = \int_0^T A'(T-z) S(z) \exp(-iq_z z) \psi(z) dz, \quad (B6)$$

which is the same as (13).

References

- BORN, M. (1942). *Rep. Prog. Phys.* **9**, 296–333.
 CASTAING, R., EL HILL, A. & HENRY, L. (1966). *C.R. Acad. Sci.* **262**, 169–172.
 CRAVEN, A. J., GIBSON, J. M., HOWIE, A. & SPALDING, D. R. (1978). *Philos. Mag.* **38**, 519–527.
 CUNDY, S. L., HOWIE, A. & VALDRE, U. (1969). *Philos. Mag.* **20**, 147–163.
 DOYLE, P. A. (1969). *Acta Cryst.* **A25**, 569–577.
 EL HILL, A. (1967). *J. Microsc. (Paris)*, **6**, 693–724.
 FERRELL, R. A. (1956). *Phys. Rev.* **101**, 554–563.
 FREEMAN, A. J. (1959a). *Phys. Rev.* **113**, 176–178.
 FREEMAN, A. J. (1959b). *Acta Cryst.* **12**, 274–279.
 GAI, P. L. & HOWIE, A. (1975). *Philos. Mag.* **31**, 519–528.
 GJØNNES, J. (1966). *Acta Cryst.* **20**, 240–249.
 HEAD, A. K., HUMBLE, P., CLAREBROUGH, L. M., MORETON, A. J. & FORWOOD, C. T. (1973). *Defects in Crystalline Solids*, **7**. Amsterdam: North Holland.
 HIRSCH, P. B., HOWIE, A., NICHOLSON, R. B., PASHLEY, D. W. & WHELAN, M. J. (1965). *Electron Microscopy of Thin Crystals*. London: Butterworths.
 HOWIE, A. (1963). *Proc. R. Soc. London Ser. A*, **271**, 268–287.
 HUMPHREYS, C. J. & WHELAN, M. J. (1969). *Philos. Mag.* **20**, 165–172.
 KAINUMA, Y. (1955). *Acta Cryst.* **8**, 247–257.
 KAMIYA, Y. & NAKAI, Y. (1971). *J. Phys. Jpn*, **31**, 195–203.
 KAMIYA, Y. & NAKAI, Y. (1976). *J. Phys. Soc. Jpn*, **40**, 1690–1697.
 KAMIYA, Y. & UYEDA, Y. (1961). *J. Phys. Soc. Jpn*, **16**, 1361–1366.
 LEAPMAN, R. D., REZ, P. & MAYERS, D. F. (1980). *J. Chem. Phys.* **72**, 1232–1243.
 MELANDER, A. (1975). *Philos. Mag.* **31**, 599–608.
 MELANDER, A. & SANDSTROM, R. (1975a). *Acta Cryst.* **A31**, 116–125.
 MELANDER, A. & SANDSTROM, R. (1975b). *J. Phys. C*, **8**, 767–779.
 NONOYAMA, M., NAKAI, Y. & KAMIYA, Y. (1973). *J. Electron Microsc.* **22**, 231–241.
 POGANY, A. P. (1971). Proc. 25th Anniv. Meeting EMAG, Cambridge, pp. 64–65.
 REZ, P., HUMPHREYS, C. J. & WHELAN, M. J. (1977). *Philos. Mag.* **35**, 81–96.
 YOSHIOKA, H. (1957). *J. Phys. Soc. Jpn*, **12**, 618–628.
 YOUNG, A. P. & REZ, P. (1975). *J. Phys. C*, **8**, L1–L7.

Acta Cryst. (1983). **A39**, 706–711

Contrast Variation of the Small-Angle Neutron Scattering of Globular Particles: the Influence of Hydrogen Exchange

BY J. WITZ

Département de Virologie, Institut de Biologie Moléculaire et Cellulaire du CNRS, 15, rue Descartes, 67000 Strasbourg, France

(Received 4 January 1983; accepted 7 April 1983)

Abstract

The influence of hydrogen/deuterium exchange on the intensity scattered by solutions of globular particles in neutron small-angle scattering experiments in $^2\text{H}_2\text{O}/$

$^1\text{H}_2\text{O}$ buffers has been calculated. By separating the contribution of the change of the average scattering density of the solute from that of the inhomogeneities of the distribution of exchangeable hydrogens, equations similar to the classical equations of Stuhrman & Kirste

[*Z. Phys. Chem. (Frankfurt am Main)* (1965), **46**, 247–250] and Ibel & Stuhrman [*J. Mol. Biol.* (1975), **93**, 255–265] are obtained. But the equations contain a contribution from the contrast-dependent fluctuations, and the geometrical parameters of the particle can no longer be simply extracted from a contrast variation study, if exchangeable hydrogens are not homogeneously distributed throughout the particle. Several examples are discussed and the potentialities of contrast variation in neutron and X-ray small-angle scattering are compared.

Introduction

X-ray diffraction at various contrasts was first used by Bragg & Perutz (1952) to determine the overall shape of the haemoglobin molecule in crystals soaked in buffers of various ionic strengths. Benoit & Wippler (1960) determined the relative organization of the components in block co-polymers from the light scattering of solutions in solvents differing by their refractive index. Recent X-ray and neutron small-angle scattering experiments have usually been based on the theory developed by Stuhrman & Kirste (1965) who showed how to separate the ‘shape function’ of a globular particle from the contribution of internal fluctuations by measuring the intensity scattered at at least three contrasts. The approach assumes that the shape and internal organization of the particle are independent from contrast. The validity of this ‘invariant volume hypothesis’ can be tested experimentally (reviewed by Luzzati & Tardieu, 1980). The assumption may hold in X-ray or neutron scattering experiments where contrast variation is achieved by addition of small molecules (sucrose, glycerol, salt, *etc.*) which usually do not penetrate either the particle or its tightly bound hydration shell. This hypothesis is incorrect in neutron scattering experiments where contrast is changed by varying the $^2\text{H}_2\text{O}/^1\text{H}_2\text{O}$ content of the solvent: the scattering density of the solute increases linearly with that of the solvent, owing to $^2\text{H}/^1\text{H}$ exchange. Ibel & Stuhrman (1975) have modified the initial equations of Stuhrman & Kirste (1965) to take this exchange into account. But they did not separate the contribution of the change of the average scattering density from that of the fluctuations around the average, although the former, for example, does not contribute to a contrast-dependent variation of the radius of gyration.

To get a better insight into the influence of the fluctuations of hydrogen exchange on the determination of the geometrical parameters of the particles of solute, we explicitly separated their contribution from that of the average scattering density. We show which basis functions and parameters can be extracted from a set of neutron scattering experiments in buffers of

various $^2\text{H}/^1\text{H}$ contents. Extension of the theory to other cases of partial permeability of the solute is trivial.

Theory

We consider a solution of identical globular particles uncorrelated in position and orientation.

\mathbf{r} and \mathbf{s} are the vectors [moduli: r (Å) and s (Å $^{-1}$)] specifying the positions in real and reciprocal space respectively. $s = (2 \sin \theta)/\lambda$, where 2θ is the angle between the scattered and incident beams, and λ the wavelength (Å). We assume that the intensity has been measured down to s_{\min} such that $D_M s_{\min} \ll 1$, where D_M is the maximal diameter of the particle.

ρ_s is the scattering density of the solvent.

$\rho_1(\mathbf{r}, \rho_s)$ is the scattering density of a particle immersed in the buffer ρ_s . Its average value is $\rho_1(\rho_s)$.

$v_1(\mathbf{r})$ is the shape function of the particle: $v_1(\mathbf{r}) = 1$ inside the particle [where $\rho_1(\mathbf{r}, \rho_s) \neq \rho_s$] and $v_1(\mathbf{r}) = 0$ outside. Its integral is the volume of the particle: $v_1 = \int v_1(\mathbf{r}) dv_r$. $v_1(\mathbf{r})$ is independent of ρ_s if $\rho_1(\mathbf{r}, \rho_s)$ varies linearly with ρ_s .

The intensity scattered by a particle arises from the fluctuations of the difference of the scattering densities of the solute and solvent:

$$\Delta\rho_1(\mathbf{r}, \rho_s) = \rho_1(\mathbf{r}, \rho_s) - \rho_s v_1(\mathbf{r}). \quad (1)$$

It is convenient to take the origin of exchange at the isopycnic point, where $\overline{\rho_1(\mathbf{r}, \rho_s)} = \rho_s = \rho_I$, and to modify (1):

$$\Delta\rho_1(\mathbf{r}, \rho_s) = \rho_1(\mathbf{r}, \rho_I) - \rho_s v_1(\mathbf{r}) + \rho_E(\mathbf{r}, \rho_I - \rho_s). \quad (2)$$

$\rho_1(\mathbf{r}, \rho_I)$ may be split into its average value $\rho_I v_1(\mathbf{r})$ and the fluctuations $\rho_{FI}(\mathbf{r})$ around this average: $\rho_{FI}(\mathbf{r}) = 0$. The contrast-dependent contribution to the scattering density, $\rho_E(\mathbf{r}, \rho_I - \rho_s)$, may also be separated into its average value $\overline{\rho_E(\mathbf{r}, \rho_I - \rho_s)}$ and the fluctuations $\rho_{FE}(\mathbf{r}, \rho_I - \rho_s)$ around the average. Both are assumed to be proportional to the $^2\text{H}/^1\text{H}$ ratio of the buffer, or to

$$\Delta\rho = \rho_I - \rho_s \quad (3)$$

$$\begin{aligned} \rho_E(\mathbf{r}, \Delta\rho) &= \overline{\rho_E(\mathbf{r}, \Delta\rho)} + \rho_{FE}(\mathbf{r}, \Delta\rho) \\ &= -\alpha \Delta\rho \{v_1(\mathbf{r}) + v_{FE}(\mathbf{r})\}, \end{aligned}$$

where $\overline{\rho_{FE}(\mathbf{r})} = \overline{v_{FE}(\mathbf{r})} = 0$ and

$$\alpha = - \frac{\int \rho_E(\mathbf{r}, \Delta\rho) dv_r}{\Delta\rho v_1} \quad (4)$$

is the ratio of the number of exchangeable hydrogens in the particle and in the volume v_1 of unperturbed solvent. The sign of the second member of (4) has been chosen to have $\alpha > 0$, since exchange increases with increasing ρ_s , or decreasing $\Delta\rho = \rho_I - \rho_s$.

So $\Delta\rho_1(\mathbf{r}, \rho_s)$ may be written

$$\Delta\rho_1(\mathbf{r}, \rho_s) = (1 - \alpha) \Delta\rho v_1(\mathbf{r}) - \alpha \Delta\rho v_{FE}(\mathbf{r}) + \rho_{FI}(\mathbf{r}) \quad (5)$$

and the structure factor of the particle is

$$f_1(\mathbf{s}, \rho_s) = \Delta\rho \{ (1 - \alpha) f_{1,v}(\mathbf{s}) - \alpha f_{FE}(\mathbf{s}) \} + f_{FI}(\mathbf{s}). \quad (6)$$

$f_{1,v}(\mathbf{s})$, $f_{FE}(\mathbf{s})$ and $f_{FI}(\mathbf{s})$ are the Fourier transforms of $v_1(\mathbf{r})$, $v_{FE}(\mathbf{r})$ and $\rho_{FI}(\mathbf{r})$, respectively.

Since $f_{FI}(0) = f_{FE}(0) = 0$ and $f_{1,v}(0) = v_1$, the variation of the square root of $i(0, \rho_s)$ with $\Delta\rho$ is linear:

$$\{i_1(0, \rho_s)\}^{1/2} = f_1(0, \rho_s) = (1 - \alpha) v_1 \Delta\rho. \quad (7)$$

The intercept with the $\Delta\rho$ (or ρ_s) axis yields ρ_I , and the slope (*vs* $\Delta\rho = \rho_I - \rho_s$) yields the effective volume $v_c = (1 - \alpha) v_1$ (Ibel & Stuhrman, 1975; Luzzati & Tardieu, 1980).

For small values of s , the scattered intensity $i_1(s, \rho_s) = \langle i_1(\mathbf{s}, \rho_s) \rangle$, averaged for all orientations of the vector \mathbf{s} , follows the Guinier (1939) law:

$$i_1(s, \rho_s) = v_c^2 \left(1 - \frac{4\pi^2}{3} R_G^2 s^2 + \dots \right), \quad (8)$$

where R_G is the radius of gyration of the particle in the solvent ρ_s . The variation of R_G^2 with the 'contrast' $\Delta\rho = \rho_I - \rho_s$ is

$$R_G^2 = R_{Gv}^2 - \frac{\alpha \mu_{2,FE}}{v_c} - \frac{\alpha^2 \mu_{1,FE}^2}{v_c^2} + \frac{1}{\Delta\rho} \left(\frac{m_{2,FI}}{v_c} + \frac{2\alpha \mu_{1,FE} \cdot \mathbf{m}_{1,FI}}{v_c^2} \right) - \left(\frac{1}{\Delta\rho} \right)^2 \frac{\mathbf{m}_{1,FI}^2}{v_c^2}, \quad (9)$$

where R_{Gv}^2 is the radius of gyration of the homogeneous particle $v_1(\mathbf{r})$, and

$$\mu_{1,FE} = \int \mathbf{r} v_{FE}(\mathbf{r}) dv_{\mathbf{r}},$$

$$\mu_{2,FE} = \int \mathbf{r}^2 v_{FE}(\mathbf{r}) dv_{\mathbf{r}}.$$

$\mathbf{m}_{1,FI}$ and $m_{2,FI}$ are the equivalent expressions for $\rho_{FI}(\mathbf{r})$. The equation resembles equation (6) of Ibel & Stuhrman (1975) but, apart from R_{Gv}^2 , it contains only terms depending upon fluctuations of the scattering density around its average value.

Since the structure factor (equation 6) is a linear function of $\Delta\rho$, the scattered intensity will be a quadratic function:

$$i_1(s, \rho_s) = \langle |f_1(\mathbf{s}, \rho_s)|^2 \rangle = (\Delta\rho)^2 A(s) + \Delta\rho B(s) + C(s)$$

$$A(s) = (1 - \alpha)^2 i_{1,v}(s) + \alpha^2 i_{FE}(s) - 2\alpha(1 - \alpha) i_{v,FE}$$

$$B(s) = 2(1 - \alpha) i_{v,FI}(s) - 2\alpha i_{FE,FI}(s)$$

$$C(s) = i_{FI}(s), \quad (10)$$

where $i_{1,v}(s)$ is the intensity scattered at unit contrast ($\Delta\rho = 1$) by the homogeneous particle $v_1(\mathbf{r})$. $i_{FI}(s)$ is the intensity scattered by the actual particle in the isopycnic solvent $\rho_s = \rho_I$. $i_{FE}(s) = \langle |f_{FE}(\mathbf{s})|^2 \rangle$, and the other functions are cross terms:

$$i_{v,FE}(s) = \langle |f_{1,v}(\mathbf{s}) f_{FE}(\mathbf{s})|^2 \rangle$$

$$i_{v,FI}(s) = \langle |f_{1,v}(\mathbf{s}) f_{FI}(\mathbf{s})|^2 \rangle$$

$$i_{FI,FE}(s) = \langle |f_{FE}(\mathbf{s}) f_{FI}(\mathbf{s})|^2 \rangle.$$

Discussion

Equations (9) and (10) are similar to the classical equations of Benoit & Wippler (1960) or Stuhrman & Kirste (1965), but each contains six unknowns (including the angle between μ_1 and \mathbf{m}_1 in (9) instead of three. However, only three basic functions can be extracted from a parabolic fit of the set of scattering curves. Neither the variation of R_G^2 with $(\Delta\rho)^{-1}$ nor that of $i(s, \rho_s)$ with $\Delta\rho$ permits one to detect that the formulas corresponding to impermeable particles are used erroneously. Nor can the difficulty be overcome by plotting the results against $\delta\rho = \overline{\rho_1(\rho_s)} - \rho_s$ instead of $\Delta\rho = \rho_I - \rho_s$: $\rho_1(\rho_s) = \rho_I - \alpha\Delta\rho$.

Using an extension of the 'invariant volume' hypothesis, Luzzati and co-workers (Appendix 1 of Luzzati, Tardieu & Aggerbeck, 1979; review by Luzzati & Tardieu, 1980) have also shown that Stuhrman's equations keep their mathematical form if the scattering density at each point \mathbf{r} is a linear function of the solvent density ρ_s . Mathematically, the volume function $v_1(\mathbf{r})$ associated with the particle is not necessarily restricted to the value 1 inside the particle [of course $v_1(\mathbf{r}) = 0$ outside], but may take any value between 0 and 1 at any point \mathbf{r} . The value and curvature at $s = 0$ of the first characteristic function [$A(s)$ in our notations, equation 10] yield the zeroth (its square, in fact) and the second moments of $v_1(\mathbf{r})$ (equations 8 and 9 in Luzzati *et al.*, 1979). These authors have also shown that the hypothesis $v_1(\mathbf{r}) = 1$ can be tested by analyzing the behavior of the autocorrelation functions corresponding to the first two Stuhrman functions [$A(s)$ and $B(s)$, equation 10], as well as by comparing small-angle scattering and pycnometric data. To determine more clearly which experimentally accessible parameter depends upon which physical property of the particle, we preferred to write directly that both the average density of the particle and the fluctuations around this average vary linearly with the scattering density of the solvent (our equations 2-4), and to calculate the structure factor and scattered intensity.

Whatever the importance of the contrast-dependent fluctuations, the third terms in (9) and (10) keep a simple significance, since they correspond to the scattering in the isopycnic solvent, where $i(0, \rho_I) = C(0)$

$= 0$ (Jacrot, 1976). It should, however, be kept in mind that a linear variation of R_G^2 with $(\Delta\rho)^{-1}$ indicates only that at the isopycnic contrast the center of the scattering density coincides with the center of volume, but does not necessarily imply that this coincidence also takes place at other contrasts.

α can, in principle, be determined from (7), if v_1 is known. In neutron scattering experiments, v_1 is usually estimated from the molecular weight and the partial specific volume of the solute. This product yields the dry volume, and its identification with v_1 neglects the possible existence of internal solvation. Internal hydration pockets very probably possess the same isotopic composition as the bulk solvent, but if they are small enough they will be seen as belonging to the particle since they contribute to the neutron scattering factor at larger angles only. If low-resolution data are collected (typically to 30–70 Å for small viruses, ribosomes, *etc.*), the volume of such pockets should be included in v_1 , at the expense of an increase of the value of α caused by their high content in exchangeable protons compared to that of protein, nucleic acid, or lipid.

In X-ray small-angle scattering experiments, the hydrated volume v_1 is readily obtained in two ways: (1) from the variation of $i(0, \rho_s)$ with contrast (Sardet, Tardieu & Luzzati, 1976), since the average density of the particle remains unaffected by the addition of small molecules to the buffer; (2) by the ratio of the intensity scattered at $s = 0$ and the total scattered intensity, taking into account that short-range fluctuations of the scattering density of quasi-homogeneous particles give rise to an additional term in Porod's law used to extrapolate $i(s)$ to large angles (Luzzati, Witz & Nicolaïeff, 1961). If the hydrated particle can be considered to be of homogeneous electron density, this method yields the volume v_1 of the particle, and if the water of hydration possesses the same electron density as that of the bulk solvent, the hydration can be calculated from v_1 and the dry volume. In the case of particles with non-homogeneous electron density, v_1 may be extracted in the same way from the characteristic function $A(s)$ (equation 10) obtained from a contrast variation study where small molecules have been added to the buffer. [Note that the hydrated volume v_1 determined from Porod's law in water or low-ionic-strength buffer might be different from the hydrated volume measured in the presence of sucrose. However, in cases where both were obtained (Le Maire, Moller & Tardieu, 1981), no measurable difference could be found.] The second technique should in principle also hold for neutron scattering in $^2\text{H}_2\text{O}/^1\text{H}_2\text{O}$ buffers, but v_1 has never been determined that way in such experiments. Indeed, neutron scattering at larger angles is usually not measured at all, and it is not known if Porod's law holds for particles where components are as segregated as in spherical viruses, for instance. It is not known either whether double-contrast variation would

actually yield the value of v_1 from the variation of the intensity at the origin: apoferritin has been investigated using double-contrast variation, but the interpretation assumes $\alpha = 0.2$, a value calculated from the chemical composition of the protein, but not determined experimentally (Stuhrman, Haas, Ibel, Koch & Chrichton, 1976).

If the exchangeable hydrogens are evenly distributed throughout the particle [$v_{FE}(r) \equiv 0$], the contribution of exchange will be fully taken into account by the term $(1 - \alpha)^2 i_{1,v}(s)$ in (10), and (9) reduces to the classical equations of Stuhrman & Kirste (1965): at infinite contrast $R_G^2(\infty) = R_{Gv}^2$. The additional terms become important if many exchangeable hydrogens are concentrated at some places only: typical values of α are: $\alpha = 0.1$ – 0.15 for proteins; $\alpha = 0.5$ – 0.6 for hydrated nucleic acids (v/v , as in the interior of spherical viruses, Jacrot, Chauvin & Witz, 1977); and $\alpha = 0.0$ – 0.07 for lipids. Furthermore, even if the influence of the contrast-dependent fluctuations is negligible in the Guinier region, it may become measurable at higher s values, where $i_{1,v}(s)$ [or $(1 - \alpha)^2 \times i_{1,v}(s)$] becomes small.

Some examples will illustrate this discussion. For a spherical particle built of a protein core (radius $R_1 = 100$ Å) surrounded by a 20 Å thick lipid shell containing no exchangeable hydrogens, R_{Gv}^2 would be overestimated by about 3% if it were identified with $R_G^2(\infty)$. Fig. 1 shows that $A(s)$ (equation 10) possesses higher subsidiary maxima than the shape function $(1 -$

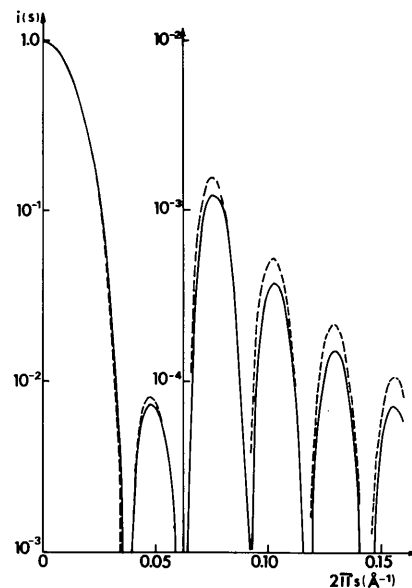


Fig. 1. Scattering curves corresponding to a spherical particle built of a core of protein (radius 100 Å) surrounded by a lipid shell (thickness 20 Å) containing no exchangeable hydrogens. — Shape function, $(1 - \alpha)^2 i_{1,v}(s)$, of the solid sphere of radius 120 Å; --- basic scattering function, $A(s)$, that would be extracted from a contrast variation study in $^1\text{H}_2\text{O}/^2\text{H}_2\text{O}$ buffers.

$\alpha)^2 i_{1,v}(s)$ and may be misinterpreted as due to a hollow sphere (hole size: about $0.1 R_2$). If the core consisted of hydrated RNA (v/v), R_{Gv}^2 would be overestimated by 15% and $A(s)$ would depart from $(1 - \alpha)^2 i_{1,v}(s)$ even more than shown in Fig. 1. Fig. 2 shows the variation of the ratio $R_G^2(\infty)/R_{Gv}^2$ for a two-shell model ($R_1 = 100$; $R_2 = 120 \text{ \AA}$) as a function of the values of the 'permeabilities' α_1 and α_2 of the inner and outer shells. $R_G^2(\infty)/R_{Gv}^2$ may differ from 1.00 (for $\alpha_1 = \alpha_2$) by as much as 30% if one shell contains much more exchangeable hydrogens than the other. Fig. 3 illustrates the variation of $R_G^2(\infty)/R_{Gv}^2$ with the ratio $\beta = R_1/R_2$ for $\alpha_1 = 0.05$ (typical for a lipid) and $\alpha_2 = 0.15$ (typical for a protein), 0.50 (typical for a hydrated nucleic acid) and 0.75. The ratio is unity at either $\beta = 0$ or $\beta = 1.0$, and passes through a maximum that becomes higher and steeper as $\alpha_1 - \alpha_2$ increases. For

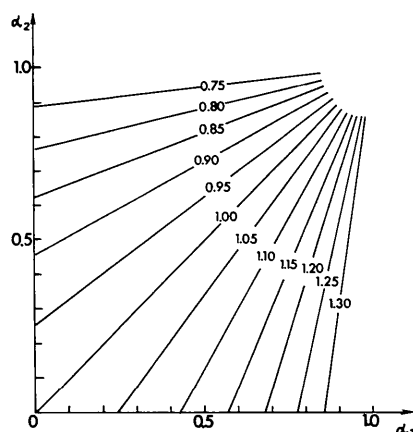


Fig. 2. Variation of the ratio $R_G^2(\infty)/R_{Gv}^2$ with α_1 and α_2 for a spherical particle made of two concentric shells of radii R_1 and R_2 ($R_2 > R_1$). $R_{Gv}^2 = 3 R_2^2/5$ is the radius of gyration of the homogeneous particle possessing the same volume. $R_G^2(\infty)$ is the radius of gyration extrapolated to infinite contrast. α_1 and α_2 represent the ratio of exchangeable hydrogens in the particle and in the same volume of solvent, for the inner and outer shells, respectively. Lines corresponding to constant values of $R_G^2(\infty)/R_{Gv}^2$ are straight lines converging to $(\alpha_1 = 1, \alpha_2 = 1)$.

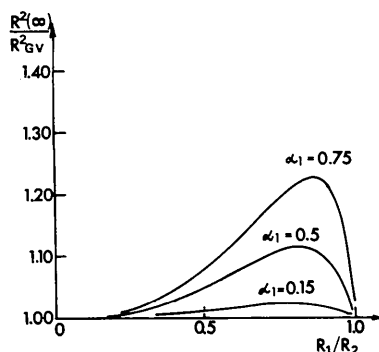


Fig. 3. Variation of the ratio $R_G^2(\infty)/R_{Gv}^2$ with the ratio $\beta = R_1/R_2$ of the inner and outer radii of the spherical two-shell model described in the caption of Fig. 2. The displayed curves correspond to $\alpha_2 = 0.05$, and $\alpha_1 = 0.15, 0.5, \text{ and } 0.75$.

particles built of concentric shells rich in nucleic acid, lipid and protein, respectively, even a larger relative difference between $R_G^2(\infty)$ and R_{Gv}^2 may be expected: it reaches about 35% for the lipid-containing Semliki Forest Virus (B. Jacrot, personal communication). Small but measurable differences between $A(s)$ and $(1 - \alpha)^2 i_{1,v}(s)$, and a 1.5% error in the determination of R_{Gv}^2 , are already expected for a model of spherical protein where hydrophilic and hydrophobic amino acids are distributed into the accessible (1/3 of the total volume) and inaccessible volumes according to the statistics of Lee & Richards (1971).

The influence of inhomogeneities of the distribution of exchangeable hydrogens is emphasized if the corresponding domains do not possess the same center, as in a particle built of two tangent spheres of the same radius R (a simplified model of the colipase-detergent complex of Charles, Sémériva & Chabre, 1980). If the scattering densities of the two moieties are those quoted in Charles *et al.* (1980), the relative difference between $R_G^2(\infty)$ and R_{Gv}^2 would be less than 0.5% and $A(s)$ and $(1 - \alpha)^2 i_{1,v}(s)$ would be identical within 1%, at least up to the second minimum of the scattering curve. But if one sphere contained no exchangeable hydrogens whereas the other one contained as many of them as does the solvent:

$$A(s) = 0.51 f_0^2(s)$$

instead of

$$(1 - \alpha)^2 i_{1,v}(s) = 0.25 f_0^2(s) \left(1 + \frac{\sin 4\pi R s}{4\pi R s} \right),$$

where $f_0^2(s)$ is the intensity scattered by a sphere of radius R . Similarly, $R_G^2(\infty) = 3R^2/5$, whereas $R_{Gv}^2 = 8R^2/5$.

For many biological molecules, a good approximation for $i_{1,v}(s)$ and R_{Gv}^2 may be obtained from neutron-scattering experiments in $^1\text{H}_2\text{O}$ buffers. This holds especially for nucleoproteins such as small spherical viruses which scatter neutrons in $^1\text{H}_2\text{O}$ buffers almost as solid spheres (Jacrot *et al.*, 1977; Chauvin, Pfeiffer, Witz & Jacrot, 1978). For a spherical particle built of a 50 Å thick protein shell surrounding a 100 Å radius core of hydrated RNA (v/v), $R_G^2(\infty) = 1.09 R_{Gv}^2$, whereas $R_G^2(\text{H}_2\text{O}) = 1.02 R_{Gv}^2$. Indeed, in many cases an important difference between $R_G^2(\infty)$ and $R_G^2(\text{H}_2\text{O})$ should be taken as an indication that exchangeable hydrogens might not be evenly distributed throughout the particle.

In model-fitting procedures such as used systematically in the study of the architecture of spherical viruses (review by Jacrot, 1981), inhomogeneities of hydrogen exchange in different regions of the particle are directly taken into account. The criteria for the validity of the model is the fit between experimental and predicted scattering curves at all contrasts, the scattering density of each region varying linearly with $\Delta\rho$.

Indeed, the slope of this variation and the isopycnic point are very different for proteins, lipids, nucleic acids, *etc.*, thus allowing the determination of the chemical composition, including solvent, of each region.

X-ray small-angle scattering is a good tool for the determination of the overall shape and size of globular particles whatever their internal structure, because the small molecules used to change the contrast are unlikely to penetrate the particle and do not give rise to additional internal-density fluctuations. Neutron scattering in $^1\text{H}_2\text{O}/^2\text{H}_2\text{O}$ buffers covering a large range of contrasts, on the other hand, provides a unique possibility to get an insight into the internal organization of complex biological particles (see also Luzzati, Tardieu, Sardet, Le Maire, Osborne & Chabre, 1983).

I thank especially Dr B. Jacrot, European Molecular Biology Laboratory Outstation, Grenoble, and Dr A. Tardieu, Centre de Génétique Moléculaire, Gif-sur-Yvette, for stimulating discussions.

References

- BENOIT, H. & WIPPLER, C. (1960). *J. Chim. Phys.* **57**, 524–527.
BRAGG, W. L. & PERUTZ, M. F. (1952). *Acta Cryst.* **5**, 277–283.

- CHARLES, M., SÉMÉRIVA, M. & CHABRE, M. (1980). *J. Mol. Biol.* **139**, 297–317.
CHAUVIN, C., PFEIFFER, P., WITZ, J. & JACROT, B. (1978). *Virology*, **88**, 138–148.
GUINIER, A. (1939). *C. R. Acad. Sci.* **208**, 894–896.
IBEL, K. & STUHRMANN, H. B. (1975). *J. Mol. Biol.* **93**, 255–265.
JACROT, B. (1976). *Rep. Prog. Phys.* **39**, 911–953.
JACROT, B. (1981). *Comprehensive Virology*, Vol. 17, edited by H. FRAENKEL-CONRAT & R. WAGNER, pp. 129–182. New York: Plenum Press.
JACROT, B., CHAUVIN, C. & WITZ, J. (1977). *Nature (London)*, **266**, 417–421.
LEE, B. & RICHARDS, F. M. (1971). *J. Mol. Biol.* **55**, 379–400.
LE MAIRE, M., MOLLER, J. V. & TARDIEU, A. (1981). *J. Mol. Biol.* **150**, 273–296.
LUZZATI, V. & TARDIEU, A. (1980). *Ann. Rev. Biophys. Bioeng.* **9**, 1–29.
LUZZATI, V., TARDIEU, A. & AGGERBECK, L. A. (1979). *J. Mol. Biol.* **131**, 435–473.
LUZZATI, V., TARDIEU, A., SARDET, C., LE MAIRE, M., OSBORNE, H. B. & CHABRE, M. (1983). *Structure, Dynamics, Interactions and Evolution of Biological Macromolecules*, edited by C. HÉLÈNE, pp. 283–298. Dordrecht, Holland: Reidel.
LUZZATI, V., WITZ, J. & NICOLAÏEFF, A. (1961). *J. Mol. Biol.* **3**, 367–378.
SARDET, C., TARDIEU, A. & LUZZATI, V. (1976). *J. Mol. Biol.* **105**, 385–407.
STUHRMAN, H. B., HAAS, J., IBEL, K., KOCH, M. H. J. & CHRISTON, R. R. (1976). *J. Mol. Biol.* **100**, 399–413.
STUHRMAN, H. B. & KIRSTE, R. G. (1965). *Z. Phys. Chem. (Frankfurt am Main)*, **46**, 247–250.

Acta Cryst. (1983). **A39**, 711–718

The Experimental Determination of the Phases of X-ray Reflections*

BY BEN POST

Physics Department, Polytechnic Institute of New York, 333 Jay Street, Brooklyn, New York 11201, USA

(Received 25 October 1982; accepted 11 April 1983)

Abstract

The application of dynamical diffraction theory to the 'phase problem' for centric crystals shows that the intensities diffracted in simultaneous three-beam interactions display characteristic maxima and minima. The sequence in which these appear on chart recordings is a sensitive function of the phase of the triplet involved in the interaction. The sequence is the same for all triplet phases of the same sign; it is reversed for those of the opposite sign. In earlier work a number of triplet phases in perfect crystals were determined. In the present work, several hundred triplet phases in mosaic crystals have been determined. Details of one of these investigations are reported in the following paper [Gong & Post (1983). *Acta Cryst.* **A39**, 719–724].

Introduction

In previous publications (Post, 1977, 1979), it was shown that the spatial distribution of the intensity diffracted by a centrosymmetric crystal in n -beam simultaneous diffraction ($n > 2$) is a sensitive function of the invariant phase of the structure-factor triplet involved in the interaction. This indicated that the signs of such phases could be retrieved directly from the diffracted intensities. Some success was finally achieved and several examples of experimental phase determination were included in the works cited above. These were based on photographic recordings of intensities transmitted through perfect and slightly imperfect thin crystals of germanium and aluminum oxide.

A major objective of the present work involves the demonstration that similar phase effects may be displayed in n -beam diffraction by *mosaic* crystals, comparable in quality, or lack of it, to crystals commonly used in crystal structure investigations. This

* This work was supported by the National Science Foundation and by the Joint Services Electronics Program of the Defense Department.